We are IntechOpen,
the world's leading publisher of
Open Access books
Built by scientists, for scientists

6,000
Open access books available

148,000
International authors and editors

185M
Downloads

Our authors are among the

154
Countries delivered to

TOP 1%
most cited scientists

12.2%
Contributors from top 500 universities

CLARIVATE ANALYTICS

BOOK CITATION INDEX

INDEXED

WEB OF SCIENCE™

Selection of our books indexed in the Book Citation Index
in Web of Science™ Core Collection (BKCI)

Interested in publishing with us?
Contact book.department@intechopen.com

Numbers displayed above are based on latest data collected.
For more information visit www.intechopen.com

Chapter

Cytotoxicity Studies of Fruit-Extracted Metal Nanostructures

Emusani Ramya and D. Narayana Rao

Abstract

Biosynthesized silver (Ag) and gold nanoparticles (Au NPs) were synthesized by using *Punica granatum* and *Citrus reticulata* extracts and these extracts act as stabilizer. The average sizes of the Silver and Gold NPs were in the range of 8–10 nm and 30–40 nm, respectively. The confirmation of NPs was done by UV-visible absorption spectra, X-ray diffraction (XRD), transmission electron microscope (TEM), and Fourier transform infrared spectra (FTIR) techniques. The luminescence studies of europium and samarium complexes with NPs were studied. Emission intensities of complexes with the presence of silver enhanced and quenched with gold due to the reabsorption. The toxicity and antimicrobial studies of nanostructures were studied.

1. Introduction

Nanomaterials exhibit chemical, physical, and biological features that are not found in other materials. In the food industry, electrical and chemistry industry, and cosmetics industry metal nanostructures have unique applications. In medicinal and industrial uses, Ag and Au nanoparticles comprise the backbone. The food sector [1, 2], catheters [3], dressings of wound [4], surgery equipment [5], synthetics [6], and optical limiter applications [7] all use silver nanostructures. Sensors [8], catalytic [9], and electrical applications [10] are only a few of the applications for gold nanoparticles. The usage of Au and Ag nanostructures as drug delivery systems demonstrated as bactericidal against Gram-positive and negative [11].

By-products from traditional synthesis techniques can be hazardous [12]. As a result, a variety of environmental and green synthesis strategies are being researched [7, 13]. Nanomedicine has had a huge influence as a result of these biosynthesized nanomaterials, and they have become the elementary units for upcoming medications to treat many ailments [14]. Plant extracts, enzymes, fungi, bacteria, and other eco-friendly synthesis processes have been using to synthesize Ag NSa and Au NSs [7, 15, 16]. Papaya, tansy, and citrus fruits are antioxidants found in fruit extracts that are used as stabilizers in the production of Ag and Au NPs [17].

Pomegranate is the scientific name for *Punica granatum*, it related to the Lythraceae's family. Polyphenol, anthocyanidins, glucose, ellagic acids, cyanidin 3-glucose, and 3,5-diglucose, hydrolysable tannins, and gall tannins, are all found in pomegranate extract [18]. Anthocyanins, which are found in abundance in pomegranates, are responsible for forming, reducing, and stabilizing of nanostructures [19]. The orange, *Citrus reticulata*, is high in phytochemicals, flavonoids, phenols, vitamins, folic acids, essential oils, and pectin [20]. Flavonoids aid in the removal of metallic ions from the body.

Ag NSs have exceptional antibacterial action, which explains why so much work is being put into developing these nanostructures. The use of Ag NPs in medicine is becoming more common. Various investigations have found that Ag NPs significantly reduce mitochondrial activity, resulting in cell apoptosis or necrosis in a variety of cells [21–23]. Interactions between Ag NPs and cells, on the other hand, have been limited. The surfaces of Au NPs are modified by DNA and amino acids when they are coupled with thiol and amine groups [24, 25]. The biocompatibility of Au NPs in therapeutic applications is critical. The size, shape, and surface modification of Au NPs determine whether they are hazardous or benign to cells [26].

Due to larger Stokes shift, narrower bandwidth of emission, and longer lifetimes emission, lanthanide ions have attracted for various applications like bio-labeling and optical amplification [27], solar cells [28], light-emitting diode (LED) [29], cancer photodynamic therapy [30], and fluoroimmunoassay [31].

Many scientists are interested in the metal enhanced fluorescence (MEF) of metal NSs and rare-earth ions because they need significantly low input intensities, and hence their applications in diagnostics have increased [32, 33]. The fluorophore's emission intensity is increased by 10–103 when it is near metal particles with subwavelength sizes [34]. The MEF is caused by two methods: (1) fluorophores' coupling with SPR, and (2) fluorophores' coupling to the SPR. The influence of a local electric field [35]. Fluorophores with metal particles at 10 nm spacing are acted on by increasing electric fields surrounded the particles, increasing their absorption cross-section and, ultimately, enhanced radiation. The energy transmits from surface plasmonic resonance to the rare-earth ion, and vice versa, results in either enhanced reduction or reabsorption in emission in the other mechanism. The fluorescence increase is primarily influenced by the shape and diameter of nanostructures, fluorophore's dipole orientations, and the overlap of the fluorophore luminescence intensity and absorption with the plasmonic band of nanostructures [36]. Because of the rivalry of the highly enhanced field surrounding nanoparticles and nonradiative transition due to the dampening of dipole oscillators by metal surfaces, MEF is mostly dependent on the spacing among metal structures and fluorophores [37].

The SPR value is altered by different shapes, various sizes, and dielectric functions of NSs as well as the host [38]. The optimal spacing between fluorophore ions and NPS for emission enhancement exists. Based on the different energy between the rare-earth ions and the metal SPR, quenching of luminescence may occur even at relatively short distances. The number of NSs, SPR, and number of phonon states of fluorophores all affect the luminescence efficiency. The plasmon-mediated augmentation of luminescence-based on the antenna effect has been found, it boosts the excitation effect and emission rate [39]. Metal nanoparticles (donor) absorb energy, which is subsequently transferred nonradiatively to rare-earth ions (acceptor) in the Forster process [40]. One group concluded that energy transmit is the primary cause of emission amplification near metal objects [41]. Other research has found that nanoparticles can stop rare-earth ions from transferring non-radiative energy to

metal nanostructures [42, 43]. These are dependent on the luminophore-nanoparticle distance, nanoparticle size, and metal particle concentration.

The goal of this research is to investigate the binding of enhanced fluorescence from Eu(TTFA)3 and Sm(TTFA)3 complexes to metal nanostructures such as silver and gold NSs in greater detail. We discovered a robust link among SPR of NSs and rare-earth molecules, as well as metal nanoparticle reabsorption by the SPR. The MTT assay is being used to investigate the cytotoxicity of metal NSs on cancer cell lines. The findings could aid in the development of biomedication delivery systems that are less hazardous than toxic ones.

2. Materials and synthesis methods

2.1 Materials

Sigma Aldrich provided silver nitrate ($AgNO_3$) and chloroaurate ($HAuCl_4$), which were used without additional purification. The *C. reticulata* and *P. granatum* were purchased from a local market. The National Centre for Cell Science (NCCS), Pune, India, provided human lung carcinoma (A549) and colorectal carcinoma (HCT116) cell lines.

2.2 Fruit extracts

Fresh *C. reticulata* and *P. granatum* peels were gathered and carefully rinsed with distilled water. A beaker was filled with 100 ml of distilled water and 6 mg of sliced *P. granatum* and *C. reticulata* fruit peels. The combination was squashed, and the extracted peel solution and strained using filter paper (Whatman no.1). Extracts were filtered again using 1.0 m filter paper to eliminate tiny particles. Then extracts were stored at 4 °C.

2.3 Synthesis of NSs

30 ml of 1 mM $AgNO_3$/$HAuCl_4$ aqueous solution was produced, and 6 ml of extracts were mixed to the 30 ml of solution at 24°C. The solution was first colorless, then progressively turned ashy, indicating the formation of Ag NPs. In the instance of Au NPs, the yellow solution turned ruby red, it showed that the forming of Au NPs. It is conducted three times to ensure that it is repeatable.

2.4 MTT assay

The MTT (3-(4,5-dimethylthiazol-2-yl)-2,5-diphenyltetrazolium bromide) test was used to investigate the cytotoxic effects of Ag NPs and Au NPs on A549 (lung) and HCT116 (colon) cancer cells. In a 96-well plate, the cell lines were plated at a density of 1×104 cells/well in DMEM/1% FBS. For 24 h, cells were incubated at 37°C in an environment of air and CO2 (95% + 5%). When the cells had reached around 80% confluence, they were treated with Ag NPs and Au NPs in various concentrations of 25, 50, 75, 100, and 125 M. MTT assay was used to determine cell vitality after 24 h. MTT solution was added to each cell in a volume of 20 L and incubated for 3–4 h. The formazan was then diffused in dimethyl sulfoxide (DMSO), and optical densities were measured on an ELISA plate reader at 550 nm. As a control, cells were grown

without nanoparticles. The ratio of mean optical density to the control was calculated after the measurements were repeated twice. The following calculation was used to calculate cell viability for each well: CV = optical density (OD) of treated well/OD value of nontreated control well) × 100%. The cytotoxicity of Ag NPs and Au NPs was compared to a positive control drug, Oxaliplatin (OXP).

2.5 Antibacterial test

Antibacterial activities of Ag and Au NPs against Gram-negative (Acinetobacter *baumannii*) and Gram-positive (*E. coli*) bacteria were tested using the well diffusion method. Before the experiment, bacterial cultures were produced to 0.5McFarland standards. Pure bacterial cultures were subcultured on Luria-Bertani (LB) agar medium and swabbed onto individual plates in a uniform manner. The wells were filled with 10 mL, 20 mL, and 30 mL Ag NPs solutions, which were then left to diffuse and incubated for 24 h at 37°C. To examine the antibacterial activity, the diameter of the zone of inhibition was employed. For the sake of reproducibility, the experiments were repeated twice.

3. Experimental details

UV-vis absorbance spectra, X-ray diffraction (XRD), transmission electron microscopy (TEM), photoluminescence, cytotoxicity, and antibacterial methods were used. The NP solutions were placed in a 10 mL cuvette and their linear absorption spectra were found with a JASCO-V670 UV/VIS/NIR spectrometer with a wavelength range of 200–800 nm and a 1 nm resolution. Samples were drop casted onto carbon grids and cured at RT for transmission electron microscopy (TEM) examinations. To assess the size of the nanoparticles, the TEM investigation was performed on an FEI model TECHNAI G2 S-Twin. The NPS were analyzed using a Bruker D8 diffractometer at 40 kV, 30 mA, using Cu-K radiation at 1° min-1 scan rate and 0.02 step size across 2 = 20–80°. Eu and Sm complexes with Ag NPs and Au NPs had their photoluminescence spectra recorded on a HORIBA JOBIN YVON fluorescence spectrometer with excitation at 350 nm.

4. Results and analysis

4.1 UV-visible absorbance spectra

The surface plasmon resonance, which is the interaction between free electrons surrounded by metal nanostructures and radiation, was used to validate the formation and stability of Ag and Au NPs. Fruit extracts reduce aqueous silver and gold ions. From **Figure** 1 shows the well-dispersed formation of Ag and Au NPs, resulted in the SPR peaks were observed in the visible region in the ranges of 350–600 nm and 500–700 nm, respectively. Due to the excitation of SPR vibrations, *P. granatum* synthesized Ag and Au NPs (**Figure** 1a and **b**) and *Citrus reticulata* Ag and Au NPs (**Figure** 1c and **d**) produced respectively. The ionization of phenolic groups in fruit extract results the formation of nanostructures. For a few months, these metal nanoparticles remain stable.
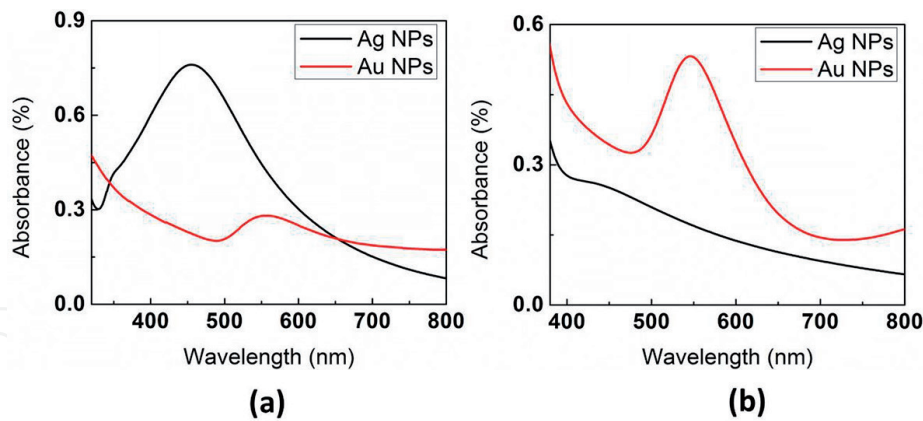
Figure 1.
Absorption spectrum of silver and gold NSs prepared by (a) Punica granatum and (b) Citrus reticulata extracts.

4.2 TEM images

The TEM images in **Figure** 2**a** and **b** shows that Ag nanostructures are in spherical shape and range in size from 30 to 70 nm (average size 62 nm). Ag NPs have crystalline FCC structure in their SAED (selected area electron diffraction) patterns. The circular planes corresponding to (1 1 1), (2 0 0), (2 2 0), and (3 1 1) match the XRD pattern very well. With a spherical dimension of 26 nm and edge length of a triangle 52 nm, Au NPs have spherical and triangular shape. Crystallinity of Au NPs with SAED patterns are shown in the planes (1 1 1), (2 0 0), (2 2 0), and (3 1 1). Similarly, the TEM images of Ag and Au NPs by citrus reticulata are shown in **Figure** 2**c** and **d**. The Ag NPs had a diameter of 56 nm and were spherical. The circular rings in the SAED pattern revealed that the produced Ag NPs were of crystalline structure. **Figure** 2**d** shows the presence of triangles in addition to spherical nanoparticles. Au NPs had a mean spherical particle size of 21 nm and a triangle edge size of 48 nm. The crystalline structure of Au NPs is revealed by the SAED pattern, which was indexed to (1 1 1), (2 0 0), (2 0 2) and (3 1 1) reflections.
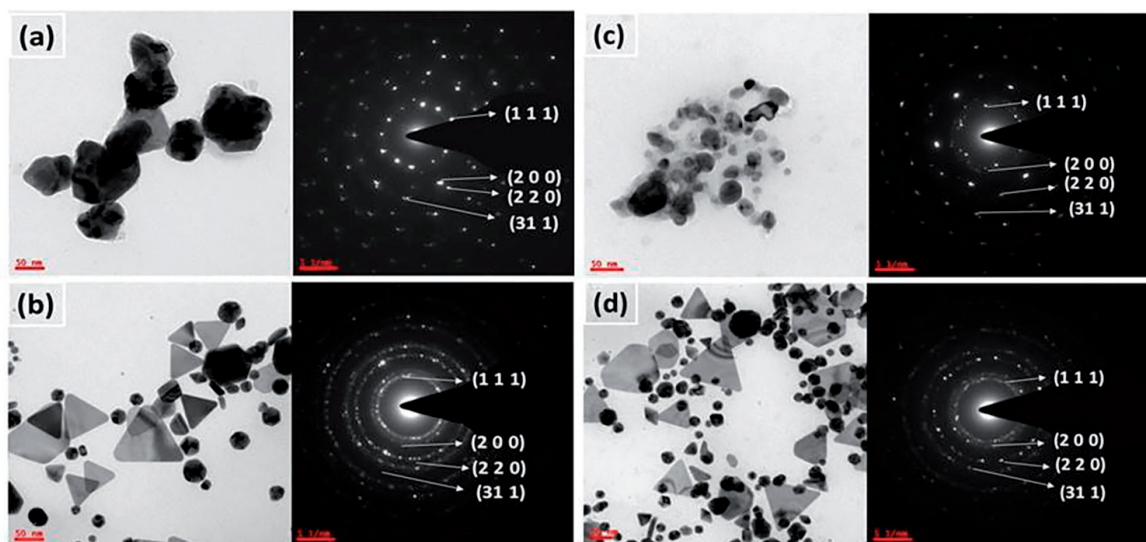

Figure 2.
TEM images and diffraction patterns of Ag and Au NSs (a) & (b) Punica granatum and (c) & (d) Citrus reticulata extract synthesized.
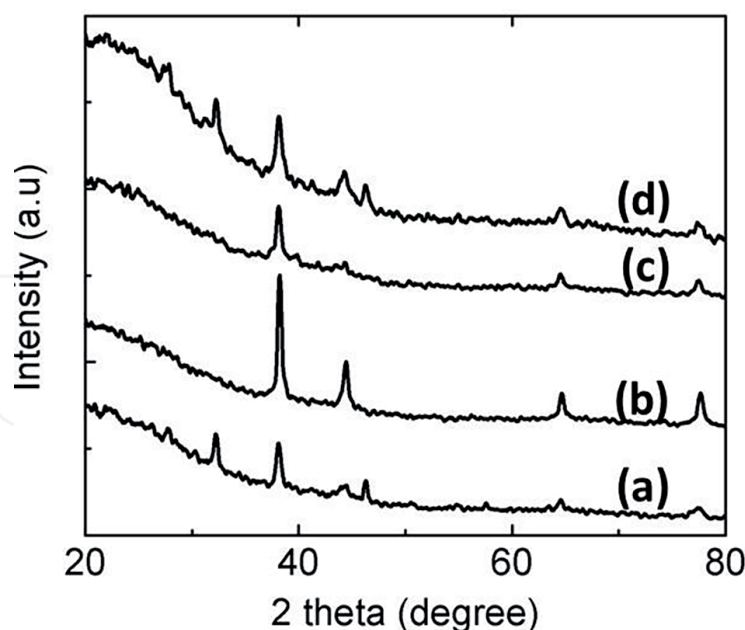
Figure 3.
XRD of Ag and Au NPs (a) & (b) Punica granatum and (c) & (d) Citrus reticulata extract synthesized.

4.3 XRD

Figure 3a–d reveals the XRD of *Punica granatum* and *Citrus reticulata* synthesized Ag and Au NSs. It shows different diffraction peaks in the range $2\theta = 20°–80°$ at 38.5°, 44.3°, 64.2° and 77.4° corresponds to (1 1 1), (2 0 0), (2 0 2), (3 1 1) planes with FCC, respectively.

4.4 Luminescence emission

In **Figure** 4**a** and **c** showed that emission of europium with Ag NPs excited at 350 nm. The Ag concentrations varied from 5 to 300 µl at 15 µl of Eu. The emission at 577 nm, 590 nm (magnetic), and 614 nm (electric) are contributing to $^5D_0 \rightarrow ^7F_0$, $^5D_0 \rightarrow ^7F_1$, $^5D_0 \rightarrow ^7F_2$ transitions respectively. These emission bands were enhanced but emission wavelengths were remains unaltered. With concentration increment of Ag, intensities increased and decreased with further increment of Ag. Similarly, **Figure** 4**b** and **d** shows the emission of Samarium with Au. The emissions at 645 nm ($^4G_{5/2} \rightarrow ^6H_{9/2}$), 566 and 602 nm ($^4G_{5/2} \rightarrow ^6H_{5/2}$ and $^4G_{5/2} \rightarrow ^6H_{7/2}$) correspond to electric and magnetic dipole transitions respectively. In the inset of **Figure** 4**b** and **d**, we show the effect of silver concentration on different transitions.

The Ag NPs' concentration dependence on the emission enhancement for $Eu(TTFA)_3$ is shown in the inset of **Figure** 4**a**, where the normalized intensity is the intensity ratio of $Eu(TTFA)_3$ solution containing Ag NPs to pure $Eu(TTFA)_3$ solution for the $^5D_0 \rightarrow ^7F_2$ transition. The luminescence enhancement gets strongly affected by the Ag NPs concentration, the maximum enhancement factor was 23 at 70 µl Ag concentration. For $^5D_0 \rightarrow ^7F_0$ and $^5D_0 \rightarrow ^7F_1$, the enhancement factor was observed as 3. The luminescence enhancement is greater for electric dipole transitions than for magnetic dipole transitions, according to this. The hyper-sensitive transition is influenced by changes in the refractive index and ligand fields around rare-earth ions caused by interactions with metal NPs [44].

The emission of rare-earth ions near NSs are affected by the near-field environment, which induces enhancement or quenching relay on the distance between nanoparticles and rare-earth ions [45]. Rare-earth ions transfer non-radiative energy to metal particles through very low distances between NPs and molecules. Because of plasmonic resonances in metal NPs, magnetic field enhancement occurs only until a certain distance [46]. More Eu ions can be closer to NSs and the distance between Eu ions and Ag NPs can be reduced by increment in number of Ag NSs. With more NPs or reabsorption of SPR, the emission intensity is quenched by energy transmit between europium and NSs. The electric dipole transition (5D0 7F2) and magnetic dipole transitions (5D0 7F0 and 5D0 7F1), on the other hand, had distinct concentration dependence on luminescence intensities. The enhancement is considered to be caused to a hard coupling between SPR and probes. **Figure** 1 shows that the absorption spectra of Ag NPs are in the wavelength range of 350–600 nm, which corresponds to the absorption of rare-earth ions. The enhancement resulted from a sensitive balance between surface Plasmon resonance reabsorption and local electromagnetic (EM) field enhancement.

Figure 4e and **g** presents the emission of 20 μl europium with Au NSs and excited at 350 nm. The emission bands at 614 nm is $^5D_0 \rightarrow {}^7F_2$ electric dipole and at 577 nm ($^5D_0 \rightarrow {}^7F_0$), and 590 nm ($^5D_0 \rightarrow {}^7F_1$) are magnetic dipole transitions. The dependency of emission of europium at 10, 20, 30 μl with gold at 5 to 300 μl is shown in the inset of
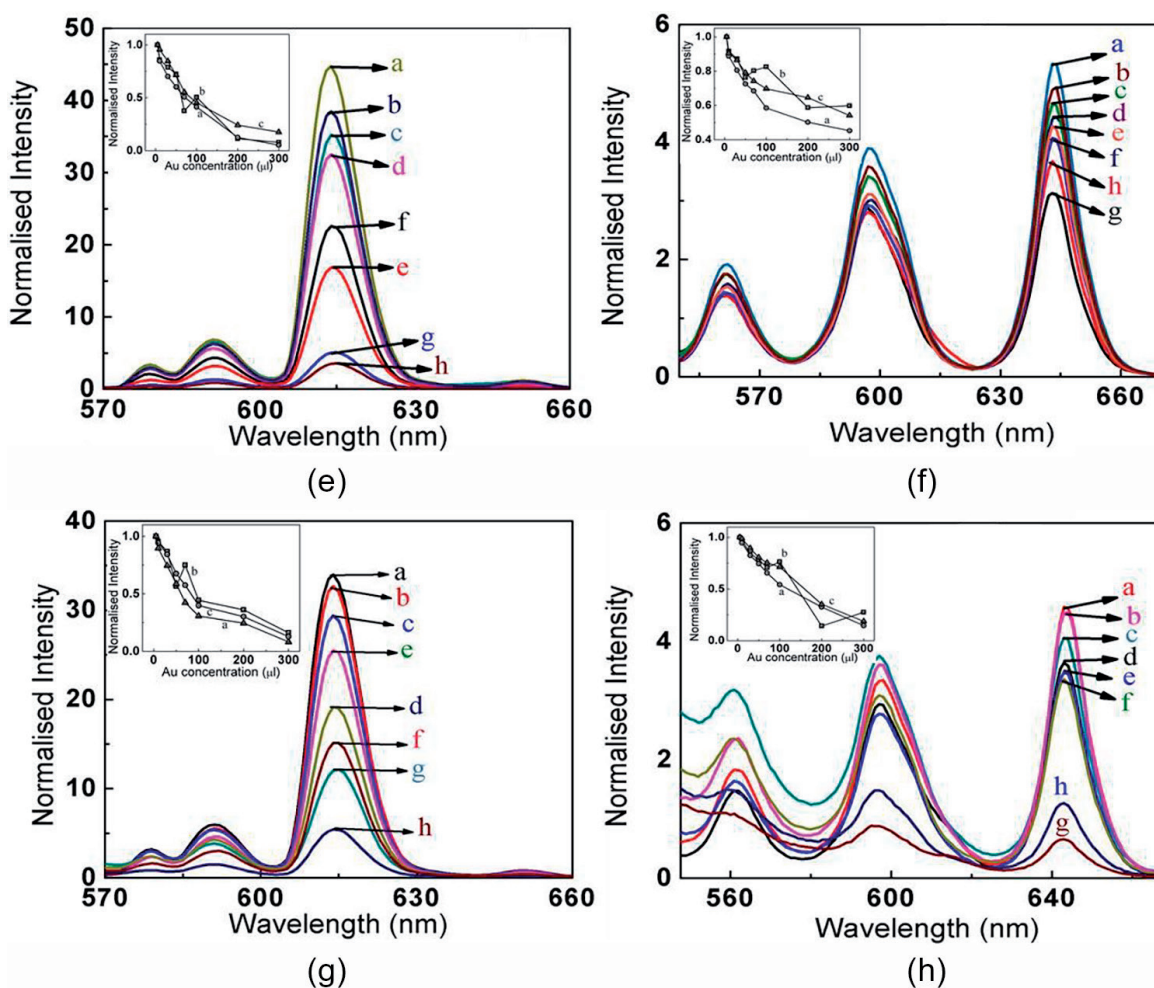

(a)

(b)

(c)

(d)
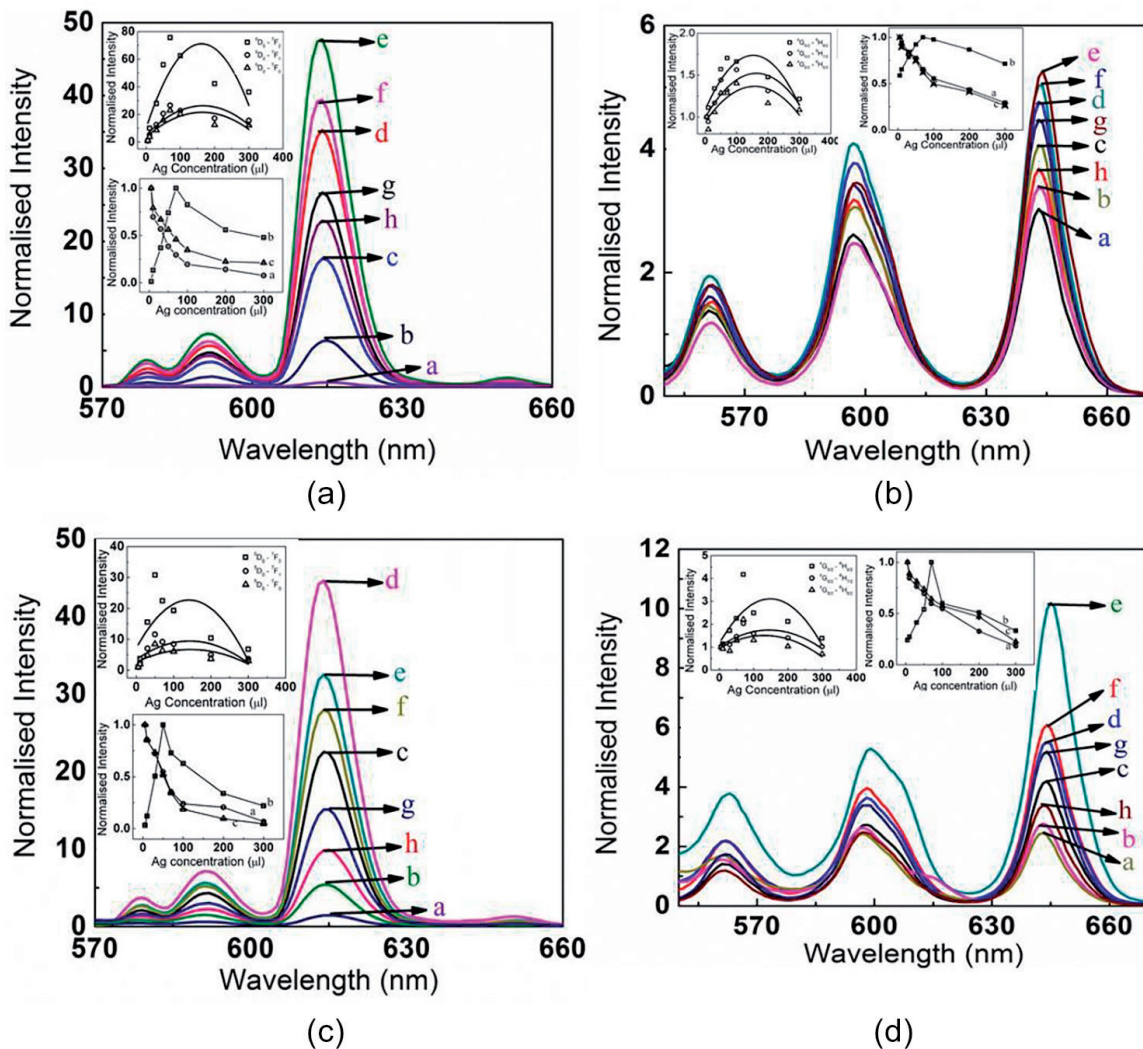
Figure 4.
((a) Punica granatum and (c) citrus reticulata) Photoluminescence of 15 μl Eu(TTFA)₃ with Ag NPs concentration: (a) 5, (b) 10, (c) 30, (d) 50, (e) 70, (f) 100, (g) 200 μl and (h) 300 μl. Inset figures: dependency of Ag with various dipole transitions and Ag concentration with emission at 10, 15, 30 μl of europium concentrations. ((b) P. granatum and (d) Citrus reticulata) Photoluminescence of 200 μl Sm(TTFA)₃ with Ag (a) 5, (b) 10, (c) 20, (d) 30, (e) 50, (f) 70, (g) 100 and (h) 200 μl concentrations. Inset figures: dependency of Ag with various dipole transitions and Ag concentration with emission at 180, 200, 220 μl of samarium concentrations. ((e) Punica granatum and (g) Citrus reticulata) Photoluminescence of 20 μl Eu(TTFA)₃ with Ag NPs concentration: (a) 5, (b) 10, (c) 30, (d) 50, (e) 70, (f) 100, (g) 200 μl and (h) 300 μl. Inset figures: dependency of Au with various dipole transitions and Au concentration with emission at 10, 20, 30 μl of europium concentrations. ((f) Punica granatum and (h) Citrus reticulata) Photoluminescence of 220 μl Sm(TTFA)₃ with Au (a) 5, (b) 10, (c) 20, (d) 30, (e) 50, (f) 70, (g) 100 and (h) 200 μl concentrations. Inset figures: dependency of Au with various dipole transitions and Au concentration with emission at 200, 220, 240 μl of samarium concentrations.

Figure 4**e** and **g**. Similarly, **Figure** 4**f** and **h** displays the emission of samarium with Au NTs. The band at 645 nm ($^{4}G_{5/2} \to {}^{6}H_{9/2}$) is an electric dipole and 566 nm ($^{4}G_{5/2} \to {}^{6}H_{5/2}$) and 602 nm ($^{4}G_{5/2} \to {}^{6}H_{7/2}$) are magnetic dipole transitions. In **Figure** 4**e** and **g** inset, emission of samarium 10, 20, 30 μl with Au at 5 to 300 μl is shown. The emission is quenched exponentially for Eu^{3+} at 10 and 30 μl and Sm^{3+} at 100 and 120 μl. The quenching is owing to the re-absorption of nanoparticles.

4.5 In vitro cytotoxicity

Green Ag and Au NTs were tested in MTT assays to see how they affected the growth of cancer cell lines. This is the first study to test the cytotoxicity of Ag NPs and Au NTs generated from *Punica granatum* and *Citrus reticulata* against cancer cells. **Figure** 5**a–d** shows the cell viability of Ag and Au nanoparticles, as well as their
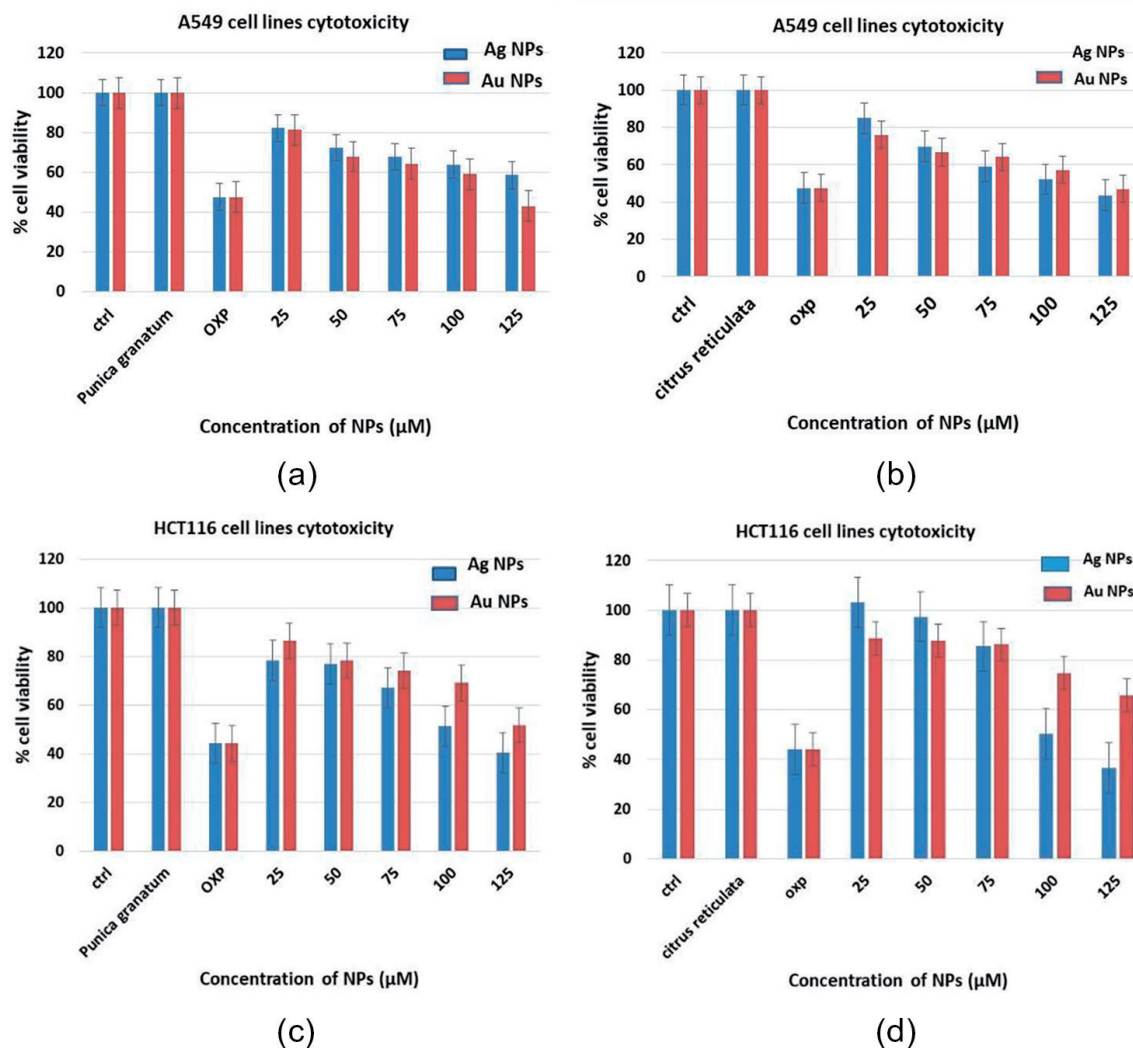
Figure 5.
Cytotoxicity studies of (a) & (b) A549 (lung cancer) cell lines of Punica granatum and Citrus reticulata and (c) & (d) HCT116 (colon cancer) cell lines of Punica granatum and Citrus reticulata of Ag NPs and Au NSs.

comparison to controls. *Punica granatum*-produced Ag and Au NPs demonstrated considerable cytotoxicity against lung and colon cancer cell lines, as shown in **Figure 5a** and **c**. *Punica granatum* produced Au NPs against lung cell lines and Ag NPs against colon cell lines, which demonstrated decreased viability of 42–40%. *Punica granatum* extract revealed no substantial toxicity, indicating that the capping agent has a minor role in toxicity. *Punica granatum*-produced Ag and Au NPs have half-maximum inhibitory concentrations (IC50) of 115 g/ml and 114 g/ml; 107 g/ml and 143 g/ml, respectively. **Figure 5b** and **d** reveals that Ag and Au NPs generated by *Citrus reticulata* are resistant to A549 and HCT116 cell lines. Cell viability decreased as the concentration of Ag and Au NPs rose. *Citrus reticulata* produced Au NPs against A549 and Ag NPs against HCT116 cell lines were found to have reduced viability, however *Citrus reticulata* extract was shown to have 100% viability. *Citrus reticulata* produced Ag and Au NPs have IC50 values of 106 g/ml and 121 g/ml; 110 g/ml and 206 g/ml, respectively.

4.6 Antimicrobial studies

Figure 6 and **Table** 1 indicate the inhibitory effect of Ag and Au NSs derived from *Punica granatum* and *Citrus reticulata* extracts. Silver nanoparticles from *Citrus*
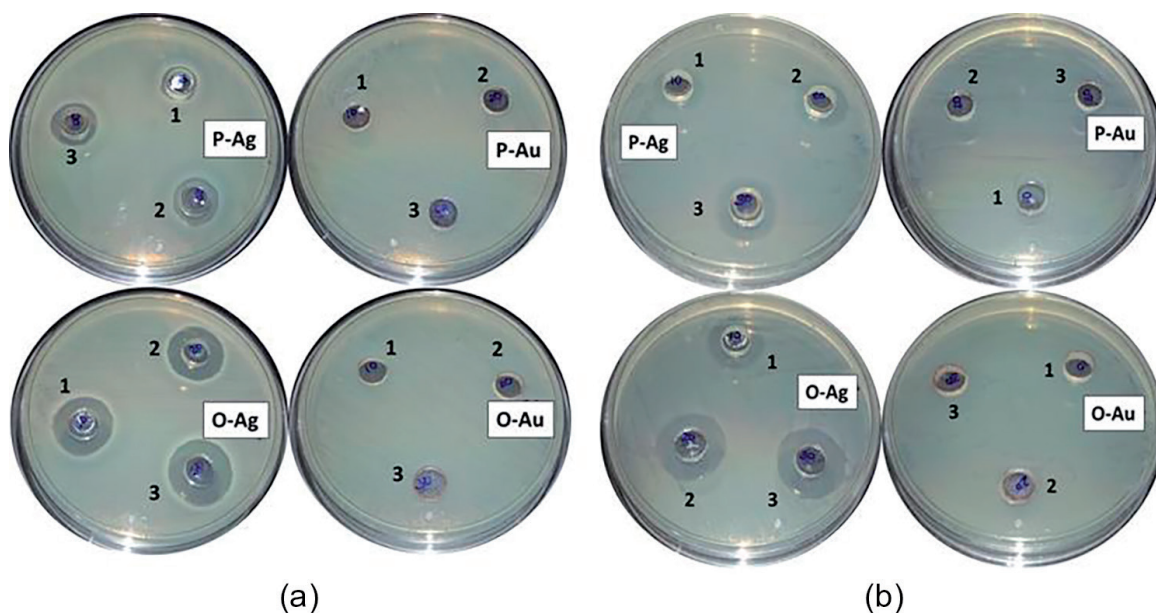
Figure 6.
Antibacterial activities of Ag and Au NPs against (a) Acinetobacter baumannii and (b) Staphylococcus aureus with (1) 10 μl, (2) 20 μl and (3) 30 μl.

Ag/Au NPs concentration (μl)		Zone of inhibition (cm)	
		A. baumannii	*S. aureus*
P-Ag	10	1.3	1.0
	20	1.5	1.5
	30	1.8	2
P-Au	10	0	0
	20	0	0
	30	0	0
O-Ag	10	2	1.8
	20	2	2.2
	30	2.5	2.4
O-Au	10	0	0
	20	0	0
	30	0	0

Table 1.
Inhibition zones of Ag and Au NSs.

reticulata extract (O-Ag) outperform *Punica granatum* silver nanoparticles (P-Ag) in these tests. However, Au NSs produced from *Punica granatum* (P-Au) and *Citrus reticulata* extracts (O-Au) had no antibacterial activity. The bacterial activity of the nanoparticles is determined by the inhibitory zones. Compared to *S. aureus*, silver nanoparticles have higher activity against *A. baumannii* (Gram-negative) (Gram-negative). The zone of inhibitions of P-Ag with10, 20, and 30 μl against Gram-negative and Gram-positive bacteria are 1.3, 1.5, 1.8 cm, and 1, 1.5, 2 cm, respectively. Similarly, for O-Ag are 2, 2, 2.5 cm, and 1.8, 2.2, and 2.4 cm against Gram-negative and Gram-negative bacteria, respectively, at different doses. When it comes to

bacterial activity, smaller particles having large surface area have greater bacterial activity than larger particles. According to the literature, cell penetration causes intracellular loss, which leads to cell death, and this inhibition is reliant on number of nanoparticles [47, 48]. The cell death is caused by silver. Due to their thin peptidoglycan coating, Ag NPs are usually more effective for Gram-negative bacteria than Gram-positive bacteria. However, in recent studies, Ag NPs have been shown to have higher antibacterial activity against Gram-positive bacteria, indicating that these Ag NPs have significantly higher antibacterial activity than other nanoparticles. Because of their small size, nanoparticles are prone to aggregation, which limits their use. In toxicity investigations, it is significant.

5. Conclusions

The effect of metal nanostructures on emission of rare-earth compounds is reported in brief research. The emission of rare-earth ions is increased initially, but then decreased when the Ag NPs concentration was increased further. The dependence of Ag NPs on emission intensity reveals a strong linkage of luminescence centers and Plasmon resonance of NSs, as well as reabsorption of SPR of Ag NPs. The anticancer and antibacterial properties of the nanoparticles were remarkable.

Conflict of interest

The authors declare no conflict of interest.

Author details

Emusani Ramya[1]* and D. Narayana Rao[2]

1 Department of Humanities and Science, CMR Institute of Technology, Hyderabad, Telangana, India

2 School of Physics, University of Hyderabad, Hyderabad, Telangana, India

*Address all correspondence to: eramya@uohyd.ac.in

IntechOpen

References

[1] Ali HRK, Moawad MS, Selim SA. In vitro study for comparing the cytotoxicity of silver and gold nanospheres on raw 264.7 murine macrophage cell line. Journal of Bacteriology Parasitology. 2016;**7**:1000264. DOI: 10.4172/2155-9597.1000264

[2] Cheng D, Yang J, Zhao Y. Antibacterial materials of silver nanoparticles application in medical appliances and appliances for daily use. China Medical Equipment Journal. 2004;**4**:26-32

[3] Samuel U, Guggenbichler JP. Prevention of catheter-related infections: The potential of a new nano-silver impregnated catheter. International Journal of Antimicrobial Agents. 2004;**23**:75-78. DOI: 10.1016/j.ijantimicag.2003.12.004

[4] Chen J, Han CM, Lin XW, Tang ZJ, Su SJ. Effect of silver nanoparticle dressing on second-degree burn wound. Zhonghua Wai Ke Za Zhi. 2006;**44**(1):50-52

[5] Lee HY, Park HK, Lee YM, Kim K, Park SB. A practical procedure for producing silver nanocoated fabric and its antibacterial evaluation for biomedical applications. Chemical Communications (Cambridge). 2007;**28**:2959-2961

[6] Lee HJ, Yeo SY, Jeong SH. Antibacterial effect of nanosized silver colloidal solution on textile fabrics. Journal of Materials Science. 2003;**38**:2199-2204

[7] Ramya E, Jyothi L, Rao DN. Influence of optical properties of Ag NPs from *Raphanus sativus* leaf extract on lanthanide complexes. Plasmonics. 2017;**12**:1601-1611. DOI: 10.1007/s11468-016-0424-x

[8] Chah S, Hammond MR, Zare RN. Gold nanoparticles as a colorimetric sensor for protein conformational changes. Chemistry & Biology. 2005;**12**(3):323-328

[9] Prati L, Villa A, Lupini AR, Veith GM. Gold on carbon: One billion catalysts under a single label. Physical Chemistry Chemical Physics. 2012;**14**:2969-2978. DOI: 10.1039/C2CP23405J

[10] Shipway AN, Katz E, Willner I. Nanoparticle arrays on surfaces for electronic, optical, and sensor applications. Chemical Physics Chemistry. 2000;**1**:18-52

[11] Han G, Ghosh P, Rotello VM. Functionalized gold nanoparticles for drug delivery. Nanomedicine (London, England). 2007;**1**:113-123

[12] Malina D, Agnieszka SK, Zbigniew W, Zygmunt K. Silver nanoparticles synthesis with different concentrations of polyvinylpyrrolidone. Digest Journal of Nanomaterials and Biostructures. 2012;**7**:1527-1534

[13] Ramya E, Jyothi L, Vivek Vardhan P, Sriram Gopal N, Rao DN. Optical and biomedical applications of eco-friendly biosynthesized silver nano spheres using zingiber officinale root extract. Nano Ex. 2020;**1**:010021

[14] Cruz D, Falé PL, Mourato A, Vaz PD, Serralheiro ML, Lino AR. Preparation and physicochemical characterization of Ag nanoparticles biosynthesized by Lippia citriodora (Lemon Verbena). Colloids and Surfaces. B, Biointerfaces. 2010;**81**:67-73. DOI: 10.1016/j.colsurfb.2010.06.025

[15] Kim J, Lee J, Kwon S, Jeong S. Preparation of biodegradable polymer/silver nanoparticles composite and its antibacterial efficac. Journal of Nanoscience and Nanotechnology. 2009;**9**:1098-1102. DOI: 10.1166/jnn.2009.C096

[16] Samadi N, Golkaran D, Eslamifar A, Jamalifar H, Fazeli MR, Mohseni FA. Intra/extracellular biosynthesis of silver nanoparticles by an autochthonous strain of Proteus mirabilis isolated from photographic waste. Journal of Biomedical Nanotechnology. 2009;**5**:247-253. DOI: 10.1166/jbn.2009.1029

[17] Jain D, Kumar Daima H, Kachhwaha S, Kothari SL. Synthesis of plant mediated silver nanoparticles using papaya fruit extract and evaluation of their antimicrobial activities. Digest Journal of Nanomaterials and Biostructures. 2009;**4**:557-563

[18] Gomez-Caravaca AM, Verardo V, Toselli M, Segura-Carretero A, Fernandez-Gutierrez A, Caboni MF. Determination of the major phenolic compounds in pomegranate juices by HPLC-DAD-ESI-MS. Journal of Agricultural and Food Chemistry. 2013;**61**:5328-5337. DOI: 10.1021/jf400684n

[19] Nadagouda MN, Iyanna N, Lalley J, Han C, Dionysiou DD, Varma RS. Synthesis of silver and gold nanoparticles using antioxidants from blackberry, blueberry, pomegranate, and turmeric extracts. ACS Sustainable Chemistry & Engineering. 2014;**7**:1717-1723. DOI: 10.1021/sc500237k

[20] Rafiq S, Rajkumari Kaul SA, Sofi NB, Nazir F, Nayik GA. Citrus peel as a source of functional ingredient: A review. Journal of the Saudi Society of Agricultural Sciences. 2018;**17**:351-358. DOI: 10.1016/j.jssas.2016.07.006

[21] Hussain SM, Javorina AK, Schrand AM, Duhart HM, Ali SF, Schlager JJ. The interaction of manganese nanoparticles with PC-12 cells induces dopamine depletion. Toxicological Sciences. 2006;**92**:456-463. DOI: 10.1093/toxsci/kfl020

[22] Braydich-Stolle L, Hussain S, Schlager JJ, Hofmann MC. In vitro cytotoxicity of nanoparticles in mammalian germline stem cells. Toxicological Sciences. 2005;**88**:412-419. DOI: 10.1093/toxsci/kfi256

[23] Hussain SM, Hess KL, Gearhart JM, Geiss KT, Schlager JJ. In vitro toxicity of nanoparticles in BRL 3A rat liver cells. Toxicology in Vitro. 2005;**19**:975-983. DOI: 10.1016/j.tiv.2005.06.034

[24] Jana NR, Gearheart L, Murphy CJ. Wet chemical synthesis of high aspect ratio cylindrical gold nanorods. The Journal of Physical Chemistry B. 2001;**105**:4065-4067. DOI: 10.1021/jp0107964

[25] Selvakannan PR, Mandal S, Phadtare S, Gole A, Pasricha R, Adyanthaya SD, et al. Water-dispersible tryptophan-protected gold nanoparticles prepared by the spontaneous reduction of aqueous chloroaurate ions by the amino acid. Journal of Colloid and Interface Science. 2004;**269**:97-102. DOI: 10.1016/S0021-9797(03)00616-7

[26] Devika CB, Arezou AG, Warren CWC. Determining the size and shape dependence of gold nanoparticle uptake into mammalian cells. Nano Letters. 2006;**6**:662-668

[27] Bouzigues C, Gacoin T, Alexandrou A. Biological applications of rare-earth based nanoparticles. ACS Nano. 2011;**5**:8488-8505. DOI: 10.1021/nn202378b

[28] Timmerman D, Izeddin I, Stallinga P, et al. Space-separated quantum cutting with silicon nanocrystals for photovoltaic applications. Nature Photonics. 2008;**2**:105-109. DOI: 10.1038/nphoton.2007.279

[29] McGehee MD, Bergstedt T, Zhang C, Saab AP, O'Regan MB, Bazan GC, et al. Narrow bandwidth luminescence from blends with energy transfer from semiconducting conjugated polymers to europium complexes. Advanced Materials. 1999;**11**:1349-1354

[30] Wang C, Tao H, Cheng L, Liu Z. Near-infrared light induced in vivo photodynamic therapy of cancer based on upconversion nanoparticles. Biomaterials. 2011;**32**:6145-6154. DOI: 10.1016/j.biomaterials.2011.05.007

[31] Mukkala V-M, Helenius M, Hemmilä I, Kankare J, Takalo H. Development of luminescent europium(III) and terbium(III) chelates of 2,2′:6′,2″- terpyridine derivatives for protein labelling. Helvetica Chimica Acta. 1993;**76**:1361-1378. DOI: 10.1002/hlca.19930760323

[32] Aslan K, Geddes CD. Directional surface plasmon coupled luminescence for analytical sensing applications: Which metal, what wavelength, what observation angle. Analytical Chemistry. 2009;**81**:6913-6922. DOI: 10.1021/ac900973r

[33] Eltzov E, Prilutsky D, Kushmaro A, Marks RS, Geddes CD. Metal-enhanced bioluminescence: An approach for monitoring luminescent processes. Applied Physics Letters. 2009;**94**:083901. DOI: 10.1063/1.3086283

[34] Xie F, Baker MS, Goldys EM. Enhanced fluorescence detection on homogeneous gold colloid self-assembled monolayer substrates. Chemistry of Materials. 2008;**20**:1788-1797. DOI: 10.1021/cm703121m

[35] Ray K, Chowdhury MH, Zhang J, et al. Plasmon-controlled fluorescence towards high-sensitivity optical sensing. Advances in Biochemical Engineering/Biotechnology. 2009;**116**:29-72. DOI: 10.1007/10_2008_9

[36] Geddes CD, Parfenov A, Roll D, Gryczynski I, Malicka J, Lakowicz JR. Silver fractal-like structures for metal-enhanced fluorescence: Enhanced fluorescence intensities and increased probe photostabilities. Journal of Fluorescence. 2003;**13**. DOI: 10.1023/A:1025046101335

[37] Campion A, Gallo AR, Harris CB, Robota HJ, Whitmore PM. Electronic energy transfer to metal surfaces: A test of classical image dipole theory at short distances. Chemical Physics Letters. 1980;**73**:447-450. DOI: 10.1016/0009-2614(80)80692-0

[38] Maier SA, Atwater HA. Plasmonics: Localization and guiding of electromagnetic energy in metal/dielectric structures. Journal of Applied Physics. 2005;**98**:011101. DOI: 10.1063/1.1951057

[39] Busson MP, Rolly B, Stout B, Bonod N, Wenger J, Bidault S. Photonic engineering of hybrid metal-organic chromophores. Angewandte Chemie. 2012;**51**:11083-11087

[40] Strohhöfer C, Polman A. Silver as a sensitizer for erbium. Applied Physics Letters. 2002;**81**:1414. DOI: 10.1063/1.1499509

[41] Eichelbaum M, Rademann K. Plasmonic enhancement or energy transfer? On the luminescence of gold-, silver-, and lanthanide-doped silicate glasses and its potential for light-emitting

devices. Advanced Functional Materials. 2009;**19**:2045-2052. DOI: 10.1002/adfm.200801892

[42] Anger P, Bharadwaj P, Novotny L. Enhancement and quenching of single-molecule fluorescence. Physical Review Letters. 2006;**96**:113002

[43] Kühn S, Håkanson U, Rogobete L, Sandoghdar V. Enhancement of single-molecule fluorescence using a gold nanoparticle as an optical nanoantenna. Physical Review Letters. 2006;**97**:017402

[44] Nabika H, Deki S. Surface-enhanced luminescence from Eu3+ complex nearby Ag colloids. European Physical Journal D: Atomic, Molecular, Optical and Plasma Physics. 2003;**24**:369-372. DOI: 10.1140/epjd/e2003-00165-x

[45] Aslan K, Geddesa CD. Surface plasmon coupled chemiluminescence from zinc substrates: Directional chemiluminescence. Applied Physics Letters. 2009;**94**:073104. DOI: 10.1063/1.3082175

[46] Liaw JW, Tsai HY, Huang CH. Size-dependent surface enhanced fluorescence of gold nanorod: Enhancement or quenching. Plasmonics. 2012;**7**:543-553. DOI: 10.1007/s11468-012-9341-9

[47] Panacek A, Kvítek L, Prucek R, Kolar M, Vecerova R, Pizúrova N, et al. Silver colloid nanoparticles: Synthesis, characterization, and their antibacterial activity. The Journal of Physical Chemistry. B. 2006;**110**:16248-16253. DOI: 10.1021/jp063826h

[48] Sondi I, Salopek-Sondi B. Silver nanoparticles as antimicrobial agent: A case study on *E. coli* as a model for gram-negative bacteria. Journal of Colloid and Interface Science. 2004;**275**:177-182. DOI: 10.1016/j.jcis.2004.02.012